Control of the Colloidal Stability of Polymer-Grafted-Silica Nanoparticles Obtained by Atom Transfer Radical Polymerization

Abdeslam El Harrak,[1] *Géraldine Carrot,**[1] *Julian Oberdisse,*[2] *Jacques Jestin,*[1] *François Boué*[1]

[1]Laboratoire Léon Brillouin, CEA-CNRS, UMR 012, Bât. 563, CEA Saclay, 91191 Gif-sur-Yvette, France
Fax: (+33) 01 69 08 82 61; E-mail: gcarrot@cea.fr
[2]Laboratoire des Colloïdes, Verres et Nanomatériaux, UMR 5587 CNRS/UM II, Place E. Bataillon, Université Montpellier II, 34095 Montpellier Cedex 5, France

Summary: Polymer chains are grafted from silica nanobeads. The method consists in grafting first the initiator molecules on the silica surface. Then, the polymerization of styrene or n-butyl methacrylate using Atom Transfer Radical Polymerization, is conducted. The nanoparticles are kept in solution during the whole process to avoid irreversible aggregation. The state of dispersion of the grafted silica nanoparticles is followed by Small Angle Neutron Scattering, as well as the quantity and the spatial organisation of the polymer. This is done during the functionalisation and the polymerization, but also after purification where free polymer chains are eliminated. This permits to reach a quantitative level of SANS analysis from these purified particles, which is compared to chemical data given by Size Exclusion Chromatography and Thermogravimetric analysis.

Keywords: atom transfer radical polymerization; grafting from; nanocomposites; silica nanoparticles

Introduction

Grafting polymers on nanoparticles for organic/inorganic nanocomposites has experienced an increasing interest in the last decade. The final aim of our work is the improvement of the mechanical properties given by the inclusion of nano-fillers (silica nanoparticles) in a polymer matrix.[1] In this frame, grafting of polymer chains onto the particle will improve the compatibility between the particles (silica surface is hydrophilic) and the polymer matrix (generally hydrophobic). We use the "grafting from" method, which consists in grafting, in a first stage, an initiator molecule, in order to perform, in a second stage, the polymerization from the particle surface.[2] Combining "grafting from" with controlled polymerizations techniques such as atom transfer radical polymerization (ATRP) has

 DOI: 10.1002/masy.200550824

shown to give very satisfactory results in terms of degree of grafting and control of polymer growth. It has been widely studied for planar surfaces[3,4] and few works on spherical particles have also been reported.[5,6]

We performed the functionalization onto colloidal silica nanoparticles (≈10 nm in diameter) dispersed in dimethylacetamide. One feature of the work is that for each reaction step, nanoparticles were kept in the same solvent to avoid aggregation that may occur by drying the particles or changing the solvent conditions. Small Angle Neutron Scattering (SANS) was used to check the state of dispersion through the successive reaction steps. Former measurements have been described before.[7, 11] Here, we followed a full set of the polymerization kinetics samples, with detailed chemical analysis such as size exclusion chromatography (SEC), thermo-gravimetric analysis (TGA) and SANS analysis. In particular, an ultimate purification stage yields samples whose spectra can be analysed quantitatively and the afforded values be compared to those obtained from SEC or TGA.

Synthesis of the ATRP-initiator-grafted-silica nanoparticles

The grafting of the initiator onto the silica surface was performed in two steps (Scheme 1).

Functionalisation. First, thiol-functionalization of the surface was achieved via silanization with a mercaptopropyl triethoxysilane. This step was a straight-forward reaction, easy to control.

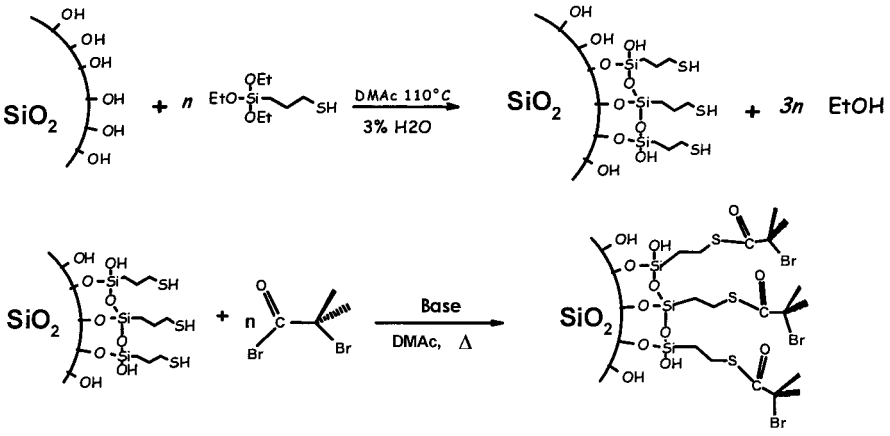

Scheme 1. Grafting of the initiator via the over-grafting method.

The use of a triethoxysilane was favored because the grafting is more efficient compared to a monoethoxysilane. Now, the drawback is the possibility to generate a polycondensed silane network. Thus, the structure of mercaptopropyl triethoxysilane (MPTS) layer onto the silica nanoparticles, depending on the degree of grafting, was investigated from ^{29}Si CP/MAS NMR. Results have been described in a previous paper.[7] In summary, we found that a monolayer was obtained up to an amount of one silane per nm^2.

Over-grafting. Second, we performed an over-grafting of the surface by reacting the thiol with 2-bromoisobutyryl bromide to generate the halogen-functional ATRP initiator. Each reaction step has been optimized to avoid aggregation of the nanoparticles. The particles were kept in the same solvent throughout the chemical process and also during the purification procedure. We never dried our particles and used ultrafiltration to clean them. Generally, from our experiments, the degree of grafting was around 0.34 initiator per nm^2.

Small Angle Neutron Scattering. SANS was used to check the state of dispersion through the successive reaction steps. This technique is particularly appropriate for such systems with colloids of 0.5 to 50 nm in size. Due to the attainable length we can check the dispersion state of the particles during all steps of the grafting, i.e., check whether the particles are aggregated or not. SANS permits also to study the structure of the final objects, and their interactions.

For a better understanding, we can simplify and describe the different features that we may obtain for spherical particles on an examplary spectrum of the scattered intensity (normalized from the concentration) versus q (Figure 1). At large angles, we expect a decrease in q^{-4} which is characteristic of a well-defined interface of hard sphere colloids. In dilute solution, the total scattered signal is proportional to the form factor of the particles. In this case, scattered curves can be analyzed with geometric models from which characteristic lengths of the system are extracted. When the concentration is increased, one can observe a structure peak which is due to particles interactions. Position of this peak gives the characteristic inter-particle distance. If, in addition, there are aggregates in the colloidal solution, their scattering may induce a strong upturns at small angles. The global size of the aggregates may be larger than the maximum size attainable in the corresponding scattering vector range. However, the scattering can still be analysed in terms of a power law of the intensity decrease; the exponent may be associated with a

compact shape (exponent -4), or be equal to the fractal dimension of the aggregates(exponent ranging between -1 and -3).

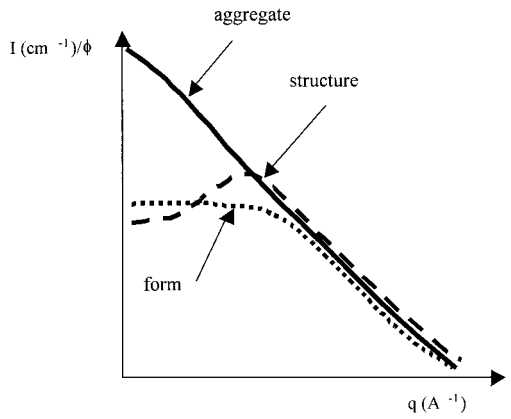

Figure 1. Typical SANS signals obtained from nanospheres in colloidal suspension.

The SANS experiments have been conducted on PACE spectrometer (LLB, Saclay). Three configurations (wavelength λ_0 = 5Å, $D_{sample\text{-}to\text{-}detector}$ = 1 m; λ_0 = 6Å, D = 3.2 m; λ_0 = 12Å, D = 4.57 m) were used, covering a q-range of 0.0035 to 0.4 $Å^{-1}$. Data treatment was carried out with a home-made program (Pasidur, LLB) following standard procedures,[8] with H_2O as calibration standard.

The SANS intensities of pure silica beads, after silanization, and after over-grafting, allowed us to verify the state of aggregation of the particles (Fig. 2a). Prior to these experiments, the initial untreated silica dispersion has been characterised in dilute conditions, Φ_{si} = 0.25 % vol. (Figure 2(b)). The initial silica particles suspension could be described as a collection of spheres with a log normal distribution centered around a mean radius value of 51 Å and a variance σ equal to 0.365 (interactions are neglected in that case, so we assume that the interparticle factor, S(q)=1).

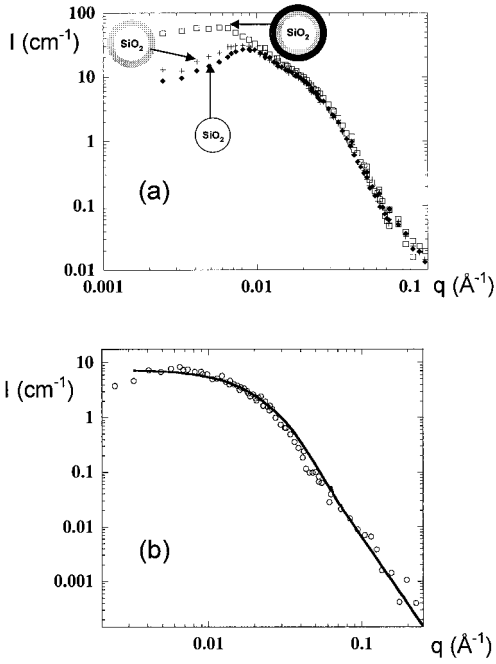

Figure 2. (a) SANS intensity from the silica dispersion at the different stages of the functionalization of the particles (Φ_{Si} = 1%): (◆) bare silica particles, (+) thiol-functional silica particles, and (□) initiator-overgrafted silica particles; (b) SANS intensity from the initial silica dispersion in DMAc (Φ_{Si} = 0.25%).

The scattering for Φ_{Si} = 1.0 % vol. of the bare silica is typical of a colloidal dispersion. Starting from low-q, the intensity first rises to a peak at q = 0.009Å^{-1}, which is the signature of repulsive interactions, presumably of electrostatic origin. At high-q, all curves show a decrease of the intensity with a q^{-4} power law as showed before in theoretical curves of Figure 1. Upon silanization, the structure was hardly modified in the q-range of observation. Once the initiator is grafted (over-grafting), there is still virtually no change at high q, whereas the intensity evolves to somehow higher values in the low-q range. This may be due to the change in the nature of the interactions. Indeed we expect to change from electrostatic interactions to steric ones. This indicates that the system may be slightly perturbed, but yet the particles remained dispersed at a whole after these two steps of the chemical modification.

"Grafting from" polymerizations

We conducted the polymerization of styrene and n-butyl methacrylate from the functionalized silica nanoparticles. The reaction was performed in the presence of free "sacrificial initiator" because of the small concentration of grafted initiator and the necessity to generate enough copper II to induce the control of the polymerization. The drawback is that it involved the presence of free chains in the solution, which would complicate the analysis.

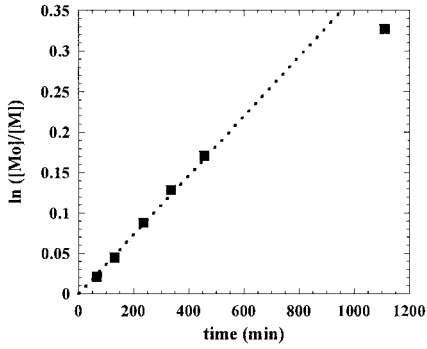

Figure 3. Semilogarithmic plot of monomer conversion versus time.

Kinetics and molecular weights analysis. The semilogarithmic plot of monomer conversion with time was linear during the whole polymerization process, attesting that a certain control has remained (Figure 3). Molecular weight of the "free" chains were found to be close to those of the grafted ones (Table 1). Free chains could be removed using centrifugation. After a first centrifugation, samples were re-dispersed in THF and this process was repeated three times, until no free chains were detected in the supernatant. Grafted polymer chains have also been analyzed from SEC (size exclusion chromatography) after etching with HF, following the procedure given by Patten.[6] Molecular weight of both the grafted polymers and the free chains were higher than expected suggesting a low initiation efficiency. This is partly explained by the steric congestion and immobilization of initiators onto the surface of the particles. Not all of the initiator sites on the nanoparticle surface have initiated the growth of polymer chains. The growing chains sterically may block the access of the catalyst to the neighbouring initiation sites on the particle surface. Similar behaviour has been observed in other works

on the polymerization from silica nanoparticles.[5,6] Nevertheless, the polydispersity index (M_w/M_n) staid low in both cases.

Table 1. SEC data for the Atom Transfer Radical Polymerization from silica nanoparticles in dimethylacetamide.

	Monomer	Conditions[a)]	No. initiator /nm^2	moles eq initiator in sol.	Reaction time (hrs)	Conv (%)[b)]	$M_{n\,SEC}$[c)]	M_w/M_n	$M_{n\,SEC}$ of cleaved chains[d)]
1	Styrene	1670:1:1:1	0.15	6.67	30	50	106600	1.55	132000 (1.28)
2	Styrene	1340:0.8:0.8:1	0.56	1.79	21	43.5	127000	1.51	144100 (1.32)
3	Styrene	775:0.6:0.6:1	0.5	6	4	5.1	32000	1.76	
4	Styrene	1460:0.6:0.6:1	0.5	3	4	8	48600	1.61	66000 (1.48)
5	Styrene	680:0.7:0.7:1	0.34	5.8	5	13.6	58080	1.5	
6	Styrene	680:0.7:0.7:1	0.34	5.8	21	28	75740	1.57	
7[e)]	n-BuMA	388:0.7:1:1	0.34	2	7	19	11200	1.15	

[a)] Conditions correspond to molar ratios of monomer, Cu(I)Br, and PMDETA, 2-bromothioisobutyrate group on the silica colloid and in solution (ratios have been calculated from values given by elemental analysis).
[b)] Conversion values are determined from gravimetric analysis.
[c)] Molecular weight of polymer chains formed in solution.
[d)] Molecular weight and molecular weight distribution in brackets, of grafted polymer chains after etching with HF.
[e)] Sample 7 has been obtained using the conditions described in the discussion, i.e., the volume fraction of n-butyl methacrylate (n-BuMA) was 40%.

Stability tests. It should be mentioned, at this stage, that the polymerization procedure had to be adapted for preserving the colloidal stability. The addition of the monomer had to be done slowly to avoid gelation of the particles. The copper was allowed to react with an excess of ligand in dimethylacetamide before the addition of the silica sol. Indeed, residual thiol that may be present at the surface of the particles (due to a non complete over-grafting) have a strong affinity with copper, leading to the formation of bridges between particles. SANS has been a privileged tool to understand the level of dispersion which is required.

We also performed polymerization of another monomer, n-butyl methacrylate (BuMA), from the same initiator-grafted-particles. Compared to styrene, the advantage of (BuMA) is its higher polarity. Hence mixtures with dimethylacetamide are more polar than styrene-DMAc ones, electrostatic particle repulsions are larger and dispersions are more stable.

The glass transition temperature (Tg) for poly(n-butylmethacrylate), around 20°C, is lower than for polystyrene (100°C) which has also an interest for us, especially with the purpose of the further step of film formation. We used similar grafting conditions, in particular with both grafted and free initiator. We obtained 20% conversion within 7 hrs. The experimental molecular weights were closer to the theoretical ones and the polydispersity was also very low (less than 1.2). The SEC and SANS characterization related to the polymerization of this monomer will be described in more details in a forthcoming paper.[9]

Thermo-gravimetric analysis (TGA). The amount of polystyrene grafted from the particles has been estimated from TGA (all samples were analyzed from the dried state, after centrifugation so as to eliminate the free chains, Table 2). An important result is that the ratio of grafted chains to free chains was somewhat lower than the initial initiator ratio (around 1/6). This ratio decreased with polymerization time, and become constant after 2 hrs (around 1/11) of polymerization.

Table 2. Thermo-gravimetric measurements of the polystyrene-grafted-silica particles

Kinetics Sample	Polymerization time	% SiO_2 residu in bulk sample	% SiO_2 residu in centrifuged sample	Grafted PS /Free PS Ratio
SiP32-2	65 min	57.66%	92.14%	1/7.5
SiP32-3	130 min	31.25%	84.55%	1/11.0
SiP32-6	455 min	7.93%	50.86%	1/11.0
SiP32-7	1110 min	7.05%	47.77%	1/11.1

The decrease could be linked to the difference in the radical concentration in the bulk and at the surface of the particles. Indeed, even if the amount of initiator was more important in the bulk, the local radical concentration around the particles was larger. However, as shown in the literature,[10] the recombination of the propagating radicals at the beginning of the polymerization (which is usually necessary for the control via the persistent radical effect) is not favoured for the grafted radicals. They cannot recombine because they are linked to the surface. But after one hour reaction, the grafted chains are long enough to be flexible so that coupling of radicals can occur. Then, the radical concentration decreases to a value low enough for the polymerization to continue in a more controlled way. These irreversible termination reactions at the beginning would induce the formation of low molecular weight chains that were detected from SEC.

At the same time, the lower polydispersity index observed for the grafted chains (main peak) compared to the free ones throughout the polymerization process, showed that the polymerization at the surface of the particles, finally proceeded in a controlled way. Moreover, it should be noted that termination reactions are much more favoured for polymer chains in solution than for chains grafted at the silica surface (due to the presence of free diffusing chains).[6]

SANS characterization of the polystyrene-grafted-silica nanoparticles

Contrast matching. SANS is also a particularly powerful tool for the characterization of the nanocomposite structure. As the density of scattering length of the solvent may be modified by mixing hydrogenated and deuterated, we can match the solvent "index" to the one of the species or of the other. The density of scattering length of silica has been determined by a contrast variation experiment (measurements at various ratios hydrogenated/deuterated).[11] In order to mask polystyrene scattering, the ratio H/D was chosen to match the scattering length density of polystyrene, ρ_{PS}, which can be calculated as usual :

$$\rho = \frac{N_{Av} \times d}{M} \times \left(\sum a_i \cdot b_i \right) \qquad (1)$$

with N_{Av} the Avogadro number, d the polymer density, M the molar mass of the statistical unit, b_i the scattering cross-section in cm^2 for each nucleus i, and a_i the number of nuclei i in one statistical unit. This value has been checked by quick contrast variation tests.

Following of the kinetics. We first analyzed the kinetics samples directly issued from the polymerization batch, without any further purification (Figure 4). Deuterated solvent (d-DMAc) has been simply added to match the scattering length density of silica. Thus, we could see only the polymer in these measurements. Note that free polymer chains were also present in the samples. The first kinetics points were taken before the polymerization started, which then corresponds to silica with no polymer. Indeed, we observe that the corresponding signal is flat and very low, identical to zero in the error bars. This proves that the silica particles were well matched. For the following kinetics points, we observe a progressive growth of the signal. The different curves displayed the same behaviour, the features of which became more and more clearly defined. Particularly striking was the presence of a shoulder at intermediate q, around 0.03 A^{-1}. At large q, the variation of I(q)

is between q^{-2} and $q^{-1.3}$, within the error bars, due to uncertainty in the solvent background subtraction. These laws correspond to the scattering from a polymer chain in good solvent at q large enough to observe the inside of the chain, i. e., at $q \rightarrow 1/\xi$, where ξ is the blob size. At intermediate q, we can see a shoulder, around 0.03 $Å^{-1}$, which seems to be more pronounced, the intensity reaches 5 cm^{-1}, at the end of the polymerization. We also observe at $q \rightarrow 0$ an increase of the curves.

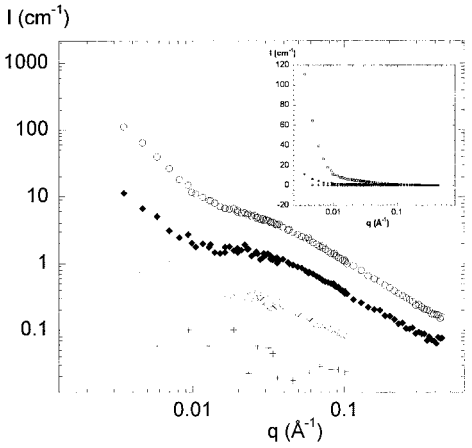

Figure 4. Evolution of the scattered intensity by samples directly taken from the polymerization batch, in silica contrast matching, at different polymerization time (the insert is semi-logarithmic plot): (+) initial time, (◊) 2 hrs, (•) 4 hrs, (Δ) 5.5 hrs, (♦) 7.5 hrs and (o) 18.5 hrs (final time).

The shapes made of an upturn followed by a rather well defined shoulder are very similar to the scattering of a shell. It could be attributed to the form factor of a shell of polymer around the silica particle, assuming no interactions between particles (see explanations above). Such interactions are likely to be visible at lower q. The q-position of the shoulder decreased slightly, due to a larger shell. This agrees with the increase of the signal with time, corresponding to the increase of the quantity of polymer around the particle. If interactions are absent, the limit at $q \rightarrow 0$ of the form factor should give a plateau which would be proportional to the mass of this shell. However, the corresponding q range is not reached here. Therefore, we cannot exclude the possibility that this increase in intensity is partly due to the signal from polymer shells of aggregates. In summary, the signal could be attributed to some shell, which increases when the polymerization proceeds. Despite of this, free chains in solution could also contribute to the scattered intensity. Because of

possible interactions between free and grafted chains, a simple subtraction of the free chains signal is tricky.

SANS on centrifuged samples. To get around this problem, SANS was performed on samples which were centrifuged as described above for separate analysis of grafted and free polymer. As before, this has been carried out in THF except for the last sample. Indeed, at the end of the polymerization, the particles exibited a so high stability in THF that centrifugation was not efficient! Then, the centrifugation had to be conducted in DMAc, which is a weaker solvent (theta solvent) than THF (good solvent).

Here again, we matched either the silica or the polymer contribution: in the different centrifuged samples, we added deuterated solvent (d-THF or d-DMAc). Evolution of the scattering curves of the hydrogenated centrifuged samples, in silica matching conditions, is presented in Figure 5 for three samples taken at different polymerization time. We can observe that the shoulder is still present, at the same q value, after extraction of free chains, attesting that this shape of the signal as well as its increase with polymerization time is only due to grafted polymer chains, not to free ones. This measurement was completed by another one for which deuterated styrene was used for the synthesis. This synthesis was strongly perturbed by aggregation, which is clearly noticeable by the increase of the intensity at low-q on Figure 5. Nevertheless, the curve evidences the shoulder, which is enhanced by the better contrast conditions due to the deuterated chains. To conclude, this result allows us to obtain an unambiguous SANS signature of the polymer layer grafted on the silica beads.

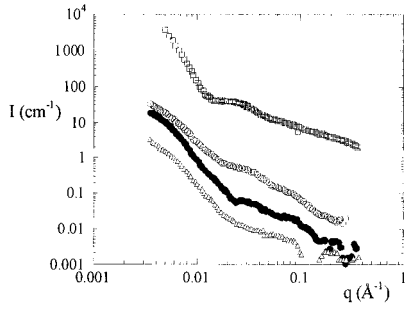

Figure 5. Scattering curves of the centrifuged hydrogenated samples, in silica matching conditions, at different polymerization time: (Δ) 4 hrs, (♦) 5.5 hrs, (o) 18.5 hrs (final time) and (□) deuterated polymer (both grafted and free chains, final time). The intensity of the deuterated one has been shifted by 100 in log scale for the sake of clarity.

Polymer matching signal. Centrifuged samples were also analysed in polymer matching conditions to follow the aggregation mechanisms during the reaction. Results for 4 hrs, 5.5 hrs and 18.5 hrs are presented on Figure 6. Data corresponds to the same silica volume fraction. We observe that all curves at large q overlap, indicating the same elementary structure of the particle at small sizes (overlap with the initial silica sol was also observed), and a good control of silica volume fraction. At the low q limit, the signal for 4 hrs and 5.5 hrs becomes much higher than for the initial sol. There was clearly some aggregation. Conversely, for the largest time (18.5 hrs) the scattering decreases again and becomes very close to the one of the initial silica sol.

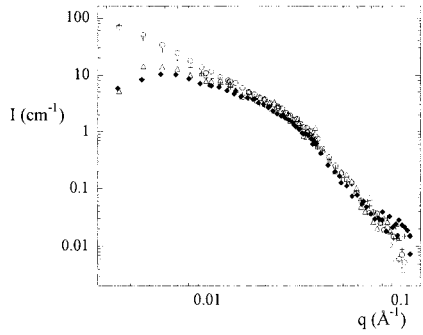

Figure 6. Evolution of the scattered intensity of centrifuged grafted particles, in polymer matching conditions, at different polymerization time: (+) 4 hrs, (o) 5.5 hrs, (Δ) 18.5 hrs and comparison with the signal of the bare beads (♦).

Thus, the first stages of the reaction were accompanied by a slight aggregation, certainly due to the change in polarity induced by the mixing of reactants (monomer, catalyst, etc…). But then particles disaggregated again as the polymerization proceeded; they have been re-stabilized by the polymer shell. This result is similar to the one shown in a previous paper [11] for the raw samples (i.e., not centrifugated). It is interesting to note that the centrifugation did not disturb the state of aggregation once the polymer was present at the surface (whereas bare silica particles would aggregate upon centrifugation).

In summary, from the polymer matching (Figure 6) scattered curves, we can just conclude that the particles were not aggregated at the end of the polymerization. After polymerization, the grafted particles are sufficiently stable so that centrifugation does not lead to aggregation. Therefore, grafted particles can be easily purified from this method.

Quantitative analysis. From the silica matching scattered curve (Figure 5, after 18.5 hrs reaction), we may then evaluate the volume of the shell from the zero q limit of the scattering, which can be expressed in absence of interactions:

$$I_0 = \frac{n}{V} \cdot \Delta\rho^2 \cdot v^2 \qquad (2)$$

where $\Delta\rho$ is the contrast between solvent and polymer shell, v is the shell volume, and

$$\frac{n}{V} = \frac{\Phi_{SiO_2}}{v_{SiO_2}} \qquad (3)$$

assuming that the number of shells per unit volume is equal to the number of particles per unit volume; Φ_{SiO_2} is the volume fraction of silica, and v_{SiO_2} the average volume of a silica particle. Linear fit of ln (I) versus q^2 gives the extrapolation value at $q \rightarrow 0$, I_0= 50 cm^{-1}. With the measured values of Φ_{SiO_2}=0.25%, v_{SiO_2}=0.889.10^6 $Å^3$, we obtain $\frac{n}{V}$=2.812.10^{15} cm^{-3}. Knowing the contrast, $\Delta\rho$=1.99.$10^{10}$$cm^{-2}$, we then find for the volume of the shell: v_{shell} = 6.70.$10^6$$Å^3$. This corresponds to a molecular weight of 4.22.10^6 g/mol. Molecular weight of the grafted chains is given by SEC, M_w = 125570 g/mol (small chains present at the surface of the particles, due to irreversible terminations at the beginning of the polymerization, have been taken into account for the calculation of M_w). So the ratio of this value with the one deduced from SANS spectra gives a calculated number of grafted chains per particles of 34.

Now, from elemental analysis, we determined a initiator grafting density of 0.34 molecules per nm^2. This gives a number of grafted initiator per particle of 137. In the present case, the overall initiation efficiency has also been calculated from the ratio of theoretical molecular weight to the experimental one, and was found to be 40%. Then, the effective number of initiator group per particle (so the maximum number of polymer chains per particle) will be equal to 55. Thermo-gravimetric analysis also permitted to evaluate the total molecular weight of the polymer shell (Table 2). The last sample gives a percentage of polymer of 53.33% which is equivalent to a shell molecular weight of 2.5.10^6 g/mol (knowing the mass of an unique particle). This corresponds to 20 chains per particle.

The difference between the value determined from SANS (34 chains) and the ones obtained from elemental analysis (55 chains) and thermo-gravimetric analysis (20 chains) is not so large, given the uncertainty of some techniques used such as elemental analysis. Moreover the calculation deduced from SANS has been evaluated from the extrapolation

of intensity at q→0, and it is probably overestimated due to the absence of a well-defined plateau. Also, the initiation efficiency has been determined for the total polymerization (i.e. both grafted and free chains are taken into account). The real value is probably less than 40% and this will then decrease the calculated number of chains.

Modelling the scattering. A refined analysis of experimental data using a hairy corona model by Pedersen[12] is under process. At the current stage of this work, it is yet difficult to fit the data with a sensible number of adjustable parameters and with a physical significance of their values. The model describes a single heary particle and it is difficult to account for many particles interactions, like agregation or repulsion, and free chains contributions. Nevertheless, a first quantitative analysis can be achieved with a simple "core-shell" model to verify the order of magnitude extracted from our other independent characterisations. The "core-shell" scattering is the average form factor of hollow spheres of inner radius R_i with a distribution p(Ri), and constant thickness e (the polymer layer). The polydispersity σ of the radii of the silica particles is taken into account by a log-normal distribution of the spheres inner radius with a R_0 maximum distribution:

$$I(q) = \frac{N}{V} \cdot \Delta\rho^2 \cdot v(Ri,e)^2 \cdot p\left(R_i, R_0, \sigma\right) \cdot \int_0^{\infty} P(q, R_i)_{couronne} \qquad (4)$$

$$P(q,R_i,e)_{shell} = \frac{9}{q^6} \times \left[\frac{\sin\left(q\left(R_i+e\right)\right) - q\left(R_i+e\right)\cos\left(q\left(R_i+e\right)\right) - \sin\left(qR_i\right) + qR_i\cos\left(qR_i\right)}{\left(R_i+e\right)^3 - R_i^3} \right]^2 \qquad (5)$$

$$p\left(R_i, R_0, \sigma\right) = \frac{1}{\sqrt{2\pi} \cdot R_0 \cdot \sigma} \times \exp\left(-\frac{\ln\left[\frac{R_i}{R_0}\right]^2}{2\sigma^2} \right) \text{ Log-normal distribution} \qquad (6)$$

with $v(R_i,e)$ the shell volume, N/V the number of shell per unit volume, Δρ the contrast between the shell and the solvent and $P(q,R_i, e)_{shell}$ the shell form factor.

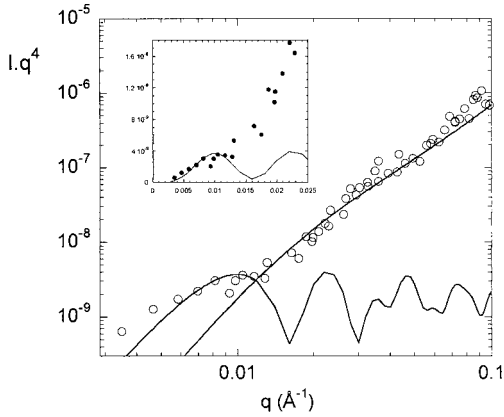

Figure 7. Analysis of grafted polymer curve (figure 5 after 18.5 hrs of polymerization) using both a "core-shell" model at low q and a Gaussian chain model at large q (in the insert: fit of the experimental linear plot with the "core-shell" model).

The result of this calculation is shown on figure 7 in a $I.q^4$ versus q plot. In the high-q region of the curve, the signal is strongly diverted from the q^4 variation and showed a q^2 variation which is certainly due to the domination of the polymer chains scattering. This is illustrated by a simulation of the scattering for the form factor of a Gaussian chain (R_g=97Å) using the Debye form factor $P(q)_{chain}$:

$$P(q)_{chain} = \frac{2\left[\exp\left(-q^2Rg^2\right)-1+q^2Rg^2\right]}{\left(q^2Rg^2\right)^2} \qquad (7)$$

To get a value of R_g, we take the molecular weight of grafted chains given by SEC, Mw=125570 g/mol, and use the well known formula $R_g=0.275*(Mw)^{0.5}$. But let us focus on the low-q region: here the q^4I vs. q plot magnifies the first oscillation of the "core-shell" form factor, and shows that it can be fitted by core-shell model with a good agreement. From the first maximum abscissa, we obtain the thickness of the shell equal to 210Å, with a size of the core corresponding to the values obtained for bare silica particles (R_0=51Å and σ=0.3). This value agrees with the length of the grafted chains, of the order of $2*R_g$=194Å.

Conclusion

We described a new route for preparing ATRP initiator-grafted-nanoparticles. In this work, we showed that every step of surface modifications and polymerization could be done while keeping the silica nanoparticles in solution. This was the best way to keep them well-dispersed and to limit the aggregation at a very moderate level. SANS measurements, looking at the silica beads distribution during the polymerization procedure, gave an understanding of the dispersion: there was a first aggregation stage induced by the mixing of the reactants, then particles disaggregated again, probably because of the repulsions between the grafted polymer layers. Looking at the polymer spatial distribution permitted to reveal the presence of a polymer layer particularly when using centrifuged samples. It even led to quantitative analysis which could be compared with the other usual characterisations. A first simple stage towards modelling is presented; progress in this direction is required and currently developed. Experimentally, the next important step is to prepare films containing these hybrid nanoparticles introduced in a matrix of the same polymer. Then, we will study the particles dispersion state in the film, first at rest, and second under stretching.

Acknowledgements

We thank France Costa-Torro (LCM, Université Pierre et Marie Curie) for the thermogravimetric analysis. We are grateful to D. Clemens for the support during the SANS experiments at BENSC (HMI, Berlin). We also thank people from Rhodia, F. Leising, C.Eychenne-Baron and M. Destarac for discussions and help. Support of this work by Région Ile de France, CEA and Rhodia is greatly acknowledged.

[1] G. Schmidt, M. M. Malwitz, *Curr. Opin. Colloid Interface Sci*, **2003**, *8*, 103.
[2] O. Prucker, J. Ruhe, *Macromolecules,* **1998,** *31*, 592.
[3] M. Husseman, E. Malmström, M. McNamara, M. Mate, D. Mecerreyes, D. Benoit, J. Hedrick, P. Mansky, E. Huang, T. Russell, C. Hawker, *Macromolecules*, **1999**, *32*, 1424.
[4] K. Matyjaszewski, P. J. Miller, N. Shukla, B. Immaraporn, A.Gelman, B. Luokala, T. Siclovan, G. Kickelbick, T. Vallant, H. Hoffmann, T. Pakula, *Macromolecules*, **1999**, *32*, 8716.
[5] J. Pyun, S. Jia, T. Kowalewski, G. D. Patterson, K. Matyjaszewski, *Macromolecules*, **2003**, *36*, 5094.
[6] T. Von Werne, T. E. Patten, *J Am Chem Soc*, **2001**, *123*, 7497.
[7] A. El Harrak, G. Carrot, J. Oberdisse, C. Eychenne-Baron, F. Boué, *Macromolecules,* **2001**, *37*, 6376.
[8] P. Lindner in: "Neutrons, X-ray and Light Scattering Methods Applied to Soft Condensed Matter", P. Lindner, T. Zemb, Eds., North Holland **2002**; p. 23.
[9] A. El Harrak, G. Carrot, J. Oberdisse, J. Jestin, F. Boué, *in preparation.*
[10] D. Xiao, M. J. Wirth, *Macromolecules*, **2002**, *35*, 2919.
[11] A. El Harrak, G. Carrot, J. Jestin, J. Oberdisse, F. Boué, *Polymer, **2005**, 46, 1095.*
[12] J. S. Pedersen, C. Svaneborg, K. Almdal, I. W. Hamley, R. N. Young, *Macromolecules*, **2003**, 36, 416-433.